



Finding the Missing Link in Methane Emission Inventories Using Aircraft and Mobile Observations

Dong Yeong Chang^{1,2} · Sujong Jeong^{1,2} · Eunsil Oh¹ · Sojung Sim¹ · Yein Kim¹ · Chaerin Park¹ · Hayoung Park¹ · Jongho Kim¹ · Jongmin Kim¹ · Jin-Soo Park³ · Hyunjae Kim³ · Jin-Soo Choi³

Received: 22 May 2021 / Revised: 2 June 2021 / Accepted: 4 June 2021 / Published online: 14 June 2021
© Korean Meteorological Society and Springer Nature B.V. 2021

Abstract

Methane emissions are associated with a wide range of human activities and contribute to climate radiative forcing as an effective absorber of terrestrial longwave radiation. In this study, we detected high levels of methane outside metropolitan areas via aircraft and mobile measurements that were conducted in February and March 2021. The emission sources were investigated using a particle dispersion model that combines the Weather Research and Forecasting model and the Stochastic Time-Inverted Lagrangian Transport model. Overall, the average measured methane emissions were 239.4–313.5 ppb (12.6–16.5%) higher than the monthly average methane levels observed at the Mauna Loa Observatory in Hawaii. In addition, methane concentration hotspots were found to be 190.2–380.8 ppb (10–20%) higher than the concentrations of the surrounding areas. According to the footprint analysis of four local methane hotspots, high methane concentrations appear to be associated with intensive pig farm areas, industrial complexes, industrial wastes dumps, and landfills. However, as there were significant methane emission sources that were hidden and thus excluded from the methane inventory, the current estimates of methane emissions may be underestimated. This study shows that more attention is needed to monitor methane leaks from both unknown and known methane emission sources. We also urge the preparation of a more reliable methane budget to achieve carbon neutrality through regular high-resolution monitoring systems.

Keywords Methane · Inventory · Metropolitan · WRF-STILT · Mobile and aircraft measurement

1 Introduction

Methane emissions are the second most important anthropogenic greenhouse gas with respect to climate change, following carbon dioxide, and act as an effective absorber of terrestrial longwave radiation (IPCC 2014). Global atmospheric methane has increased by 10% over the last two

decades, and in recent years, more drastic increases have been observed by the Global Monitoring Laboratory (GML) of the National Oceanic and Atmospheric Administration (NOAA; www.esrl.noaa.gov/gmd/ccgg/trends_ch4/). Atmospheric methane has a relatively short lifetime (about 12 years), as compared with carbon dioxide, but is a more efficient radiation absorber, making it over 20 times more potent than carbon dioxide. According to the 2019 Annual Greenhouse Gas Index published by NOAA's Global Monitoring Institute, methane accounts for 17% of the total radiative forcing caused by greenhouse gases. Therefore, to moderate global warming, methane emission sources and sinks must be investigated, and anthropogenic emission sources must be controlled. Several countries, including South Korea, the United States, China, and the European Union, have begun investigating carbon budgets and planning strict greenhouse gas emission regulations in order to achieve carbon neutrality. To regulate greenhouse gas emissions effectively, it is necessary to accurately assess

Responsible Editor: Hyo-Jong Song.

✉ Sujong Jeong
sujong@snu.ac.kr

¹ Department of Environmental Planning, Graduate School of Environmental Studies, Seoul National University, Seoul, Republic of Korea

² Environmental Planning Institute, Seoul National University, Seoul, Korea

³ National Institute of Environmental Research, Incheon, Republic of Korea

the current methane sources at both regional and national scales (Miller et al. 2013). Analysis of methane emission trends based on long-term monitoring and accurate investigation of methane cycle can help to reduce carbon budget uncertainty in anthropogenic emissions and reduce future methane emissions (Bergamaschi et al. 2018; Pacala 2010). Even though researchers have investigated methane sources and sinks for decades, there are still large discrepancies. Specifically, these discrepancies are related to a lack of observations and a dearth of understanding of the various methane processes from both natural and anthropogenic sources (Kirschke et al. 2013; Saunois et al. 2017; Turner et al. 2019).

Methane is released from both anthropogenic and natural sources. In particular, methane is emitted from wetlands, biomass and biofuel burning, termites, wild animals, and permafrost as natural sources. Meanwhile, 50–65% of the global methane budget is supplied by human activities, such as energy and industrial facilities, traffic emissions, the production and transportation of coal, gas, and oil, agriculture (e.g., livestock breeding and paddy rice cultivation), and anthropogenic waste (e.g., landfill and sewage treatment plant), especially relating to the decay of organic waste (Ciais et al. 2013; Kirschke et al. 2013; Saunois et al. 2020). These anthropogenic methane emissions are closely related to the economy, politics, culture, and the environment, and can therefore vary by country, region, and culture. Further, each country may have distinct compositions of methane emission sources because of different agricultural processes and livestock breeding conditions, which are the main anthropogenic sources of methane emissions. Regional differences in methane emissions at the local level are associated with a wide range of human activities. In rural areas, rice cultivation, biomass burning, and livestock breeding are the main sources of methane, whereas in megacities, the main sources are associated with transportation. As metropolitan areas are constantly expanding with increasing urbanization, energy consumption increases (e.g., fossil fuels and biomass burning), in addition to anthropogenic waste and methane. In particular, poorly regulated landfills require special attention to reduce atmospheric methane emissions (Nisbet et al. 2020). Currently, the carbon budget does not adequately account for the variability of methane emissions, which means that to reduce large uncertainties in the carbon budget, specific knowledge regarding the current methane sources and sinks is required.

Therefore, in this study, we investigate the suspected methane emission sources based on local methane concentration hotspots outside of South Korean metropolitan areas (Hwaseong, Pyeongtaek, Anseong, and Dangjin) via airborne and mobile measurements using a particle dispersion model. Further, we discuss the need for regular methane monitoring systems to meet carbon-neutral targets for climate change mitigation.

2 Methods

2.1 Aircraft Measurements

Aircraft measurements were conducted using a CO/CO₂/CH₄/H₂O analyzer (GLA331-MCEA1-911) onboard a Beechcraft 1900D on February 20 and 21, 2021. This analyzer can measure ambient levels of carbon monoxide, carbon dioxide, methane, and water vapor with extraordinary precision in real-time using tunable diode laser absorption spectroscopy (Off-Axis Integrated Cavity Output Spectroscopy), with precision and drift of 1 ppb and 0.1 ppm, respectively. The measurement rate was 10 Hz (0.01–10 Hz available), and the flow time response was less than 0.1 s.

2.2 Mobile Measurements

Atmospheric methane levels were monitored using a methane trace gas analyzer (LI-COR Environmental, LI-7810) during transit from urban to rural areas. The LI-7810 uses optical feedback cavity enhanced absorption spectroscopy as a laser-based measurement technique. It is suitable for monitoring methane in highly variable traffic conditions, where it is necessary to measure a wide range of methane concentrations (0 ppb to 100,000 ppb). The measurement precision (1σ) is 0.60 ppb at 2 ppm with 1 s averaging. The inlet of the methane measurement instrument was fixed to the outer part of the vehicle at a height of 1.7 m above the ground facing the opposite direction of the vehicle to minimize pressure fluctuations. The vehicle was operated at a constant speed during the measurements. The route and speed of the mobile platform were recorded every second using a Global Positioning System (GPS) device (AscenKorea, AK-770). All data were recorded in real-time every second and checked via Wi-Fi.

2.3 WRF-STILT Model for Footprint Analysis

We use a particle dispersion model that combines the Weather Research and Forecasting model (WRF) and the Stochastic Time-Inverted Lagrangian Transport model (STILT), known as WRF-STILT, to investigate the methane emission sources. The WRF-STILT can calculate the adjoint of the dispersion model in the form of a footprint field backward in time from a measurement location. The calculated footprints demonstrate the influence of upwind methane surface fluxes on major methane emission sources. In this study, we used WRF-STILT to calculate four footprint fields (i.e., one hour back from the influence area) of high methane concentrations detected by aircraft or mobile measurements.

3 Results

Figure 1 shows the airborne and mobile measurements conducted on February 20 and 22, and March 12 and 13, 2021, respectively. The column lines delineate the flight and mobile movement paths around the outer metropolitan area, and the column heights and colors denote the measured methane concentration of each path. The suspected emission sources of methane are intensive pig farm areas, petrochemical and industrial complexes, approved landfills, and non-approved landfill and dump areas, which are marked with yellow squares, red and green diamonds, and white and orange circles, respectively, in Figs. 1 and 2. Some of these sources were hidden and thus not included in the methane inventory. Overall, the measured methane concentrations ranged from 2000 ppb to 2250 ppb, with averages of 2160.0 ppb and 2239.04 ppb for the aircraft and mobile measurements, respectively. The averages of the measured methane concentrations were 12.6–16.5 % higher than the monthly averages of methane concentrations for February and March 2021, which were 1917.10 ppb and 1921.16 ppb, respectively, as observed at the Mauna Loa observatory in the United States (downloaded from NOAA/GML; www.esrl.noaa.gov/gmd/ccgg/trends_ch4/).

The local hotspots of detected methane were found to be about 200–380 ppb (about 10–20 %) higher than that of the surrounding area. Both measurements detected strong methane emission signals in similar areas located near pig farms, landfills, and industrial complexes, despite different observation periods. Outside the metropolitan area, there were

complex major methane emission sources that were closely related to urban expansion and metropolitan support activities. Herein, a combined Weather Research and Forecasting and Stochastic Time-Inverted Lagrangian Transport (WRF-STILT) model was used to calculate the footprints of methane emissions from high levels of methane concentrations (higher than 2200 ppb), as shown in Fig. 2. The results confirm that the hotspots of methane concentration are affected by the suspected methane emission sources.

High methane concentrations (higher than 2200 ppb) were observed along the aircraft measurement track from 127.234°E to 37.059°N to 37.087°N on February 20, 2021 (Figs. 1a and 2a). These methane concentrations seem to be heavily affected by methane emissions produced during the decomposition of waste in dumps and landfills. As shown in Fig. 2a, the footprints calculated by the WRF-STILT show the back trajectory of methane emissions from a non-approved landfill (marked with orange circles). The local methane emission hotspots shown in Fig. 1b were detected by aircraft measurements conducted on February 22, 2021, and appear to be associated with two main methane emission sources: intensive pig farm areas and industrial complexes along the coast and shoreline. These emission sources were also detected by mobile measurements (Fig. 1c and d). Moreover, high methane concentrations were found over the paths from urban to rural areas on March 12, 2021. Figure 2c shows the footprint of a high methane concentration that is associated with an industrial complex because of its location on the downwind side of the mobile path. Unapproved landfills, circled in white at the 37°N latitude, also

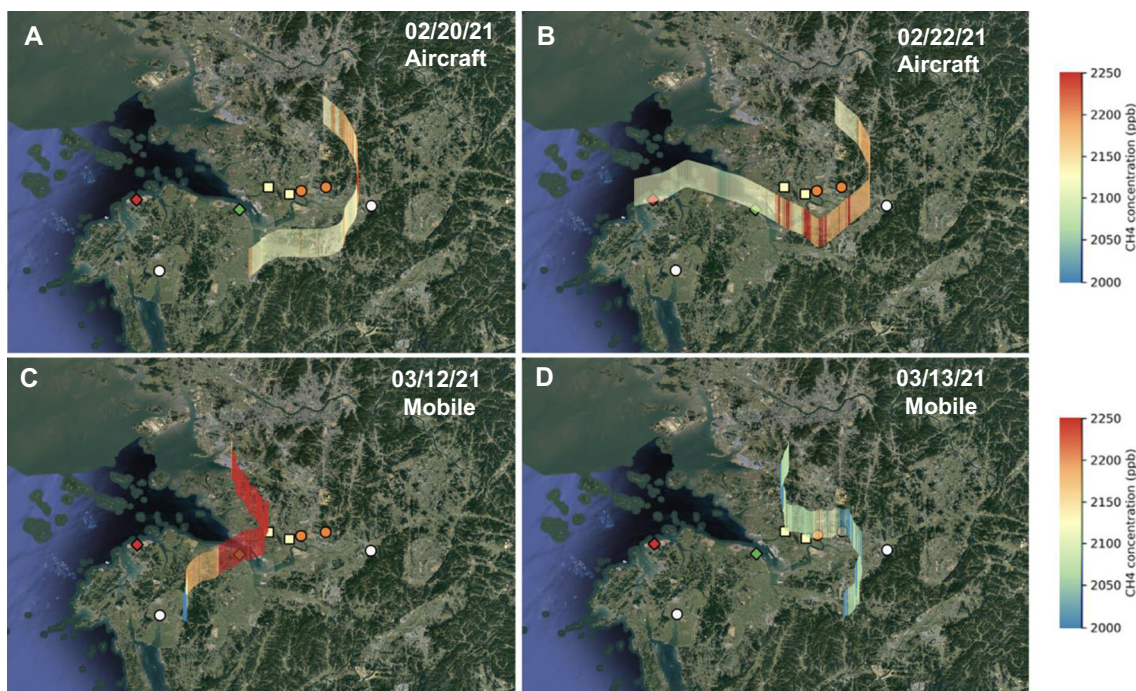


Fig. 1 Methane concentration observed by aircraft and mobile measurements (ppb); yellow squares, red and green diamonds, white and orange circles denote intensive pig farm areas, petrochemical and industrial complexes, approved landfills, and non-approved landfill and dump areas, respectively

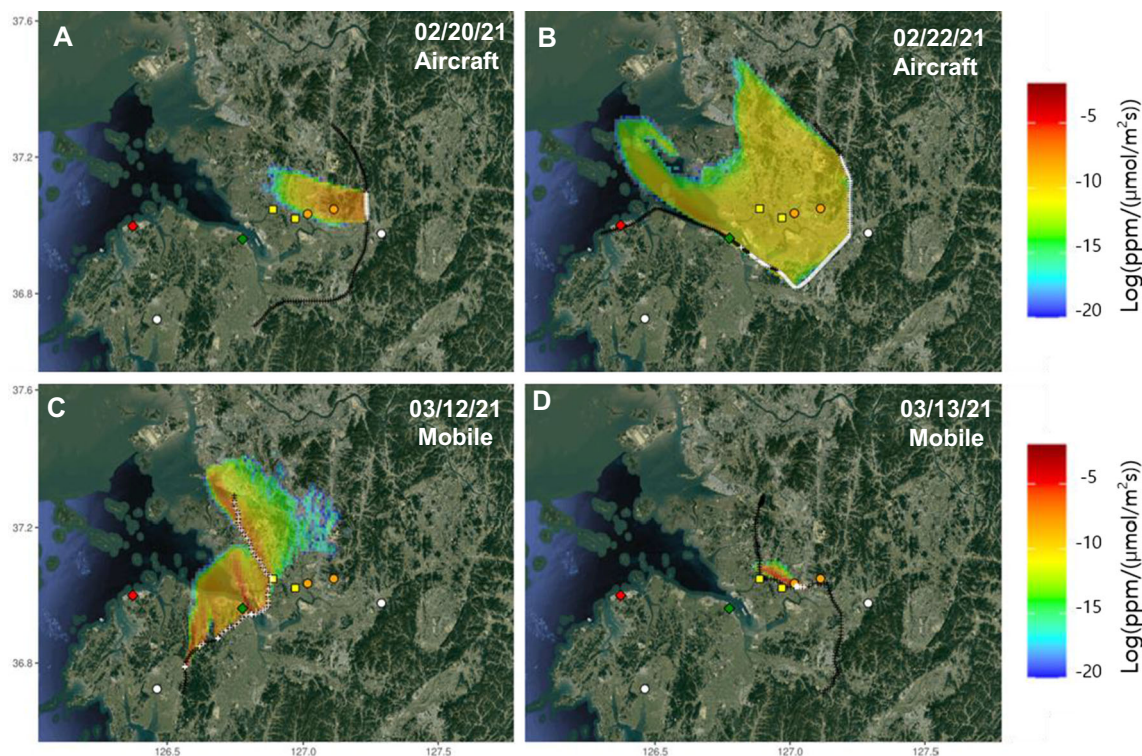


Fig. 2 Footprints of the highest methane concentrations observed during the aircraft and mobile measurements (Unintended and unknown Landfills). The black cross represents the measuring point, and the white cross represents the high concentration of methane (2200 ppb or more) used starting points for footprint calculations. The suspected

emission sources are marked by yellow squares, red and green diamonds, white and orange circles which denote intensive pig farm areas, petrochemical and industrial complexes, approved landfills, and non-approved landfill and dump areas, respectively

contributed to increasing methane concentration levels (see Fig. 2a). Meanwhile, for the petrochemical complexes, in which methane leaks are suspected, no high methane signals were detected during the study period. This may be related to the large distance between the methane source and mobile receiver, which was several kilometers from the source. In addition, the height of the mobile receiver inlet may have been positioned too low to have detected the signals.

On March 13, 2021, the footprints shown in Fig. 2d revealed isolated influencing areas near pig farms that might relate to a narrow distribution of high methane concentration (Fig. 1d), which is in contrast to the wider footprints (Fig. 2b and c). The lower concentration of methane emissions measured on March 13, 2021 seems to be affected by the efficient dispersion of atmospheric conditions. The Korea Meteorological Administration (data.kma.go.kr) provides the atmospheric dispersion index (ADI), which is a type of ventilation coefficient factor for diagnosing dispersion efficiency. The ADI values are highly dependent on the meteorological conditions (wind, temperature, and precipitation) and are calculated as 55, 62, 55, and 74 for Fig. 2a and d, respectively. The ADI on March 13 (Fig. 2d) was 20–35% higher than that on the other measurement days, which may be because of a low level of residual air pollutants as a result of high air diffusion and transport capacity.

4 Discussion

We detected high levels of methane emissions outside metropolitan areas using aircraft and mobile measurements and investigated the potential emission sources using the WRF-STILIT model. Local methane emission hotspots were detected near suspected methane source areas, including pig farms, landfills, and industrial complexes, regardless of the observation period. These are the main source of methane emissions in the metropolitan outer areas, and some of them are poorly regulated. According to the Korean methane inventory in 2018, agriculture and waste-related methane emissions accounted for 43.53 and 30.90% of the total methane inventory, respectively.

Methane emissions associated with pig farms necessitate particular attention because they can increase with income growth and expanded urbanization. Higher standards of living can lead to increased meat consumption, and as a result, livestock and intensive breeding farms may expand to meet the growing meat demand, which consequently increases methane emissions. Landfills and dumps, which are the second-largest source of methane emissions, also require particular monitoring attention in order to reduce methane emissions as they can emit significant amounts of methane but are poorly regulated. Specifically, some landfills and dumps are entirely excluded in the methane emissions inventory, which can lead

to significant uncertainty in the carbon budget. Neither the flight nor mobile observations in this study observed methane leaks from petrochemical complexes, but monitoring systems are still required as we cannot clearly determine where the methane leaks are located. Note that high-resolution satellites can be used to detect methane leaks during fossil fuel production and transportation in the United States (de Gouw et al. 2020). Overall, more attention is needed to monitor methane leaks from both known and unknown methane emission sources and sinks. Furthermore, regular monitoring systems are required as these poorly regulated methane emissions are crucial for achieving carbon-neutral goals.

Acknowledgements This work was supported by the National Research Foundation of Korea (NRF) grant funded by the Korean government (MSIT) (No. NRF-2019R1A2C3002868). Airborne data collection was supported by the National Institute of Environment Research (NIER), funded by the Ministry of Environment (MOE) of the Republic of Korea (NIER-2020-01-01-010).

References

- Bergamaschi, P., DANILA, A.M., Weiss, R., Thompson, R.L., Brunner, D., Levin, I., meijer, Y., Chevallier, F., JanssensMaenhout, G., Bovensmann, H., Crisp, D., Basu, S., Dlugokencky, E.J., Engelen, R., Gerbig, C., Günther, D., Hammer, S., Henne, S., Houweling, S., Karstens, U., Kort, E.A., Maione, M., Manning, A.J., Miller, J., Montzka, S., Pandey, S., Peters, W., Peylin, P., Pinty, B., Ramonet, M., Reimann, S., Röckmann, T., Schmidt, M., Strogies, M., Sussams, J., Tarasova, O., Van Aardenne, J., Vermeulen, A., Vogel, F.: Atmospheric monitoring and inverse modelling for verification of greenhouse gas inventories, EUR – Scientific and Technical Research Reports, Publications Office of the European Union, available at: <https://ec.europa.eu/jrc/en/publication/eur-scientific-and-technical-research-reports/atmospheric-monitoring-and-inversemodelling-verification-greenhouse-gas-inventories>. Accessed 17 Mar 2020 (2018)
- Ciais, P., Sabine, C., Bala, G., Bopp, L., Brovkin, V., Canadell, J., Chhabra, A., DeFries, R., Galloway, J., Heimann, M., Jones, C., Quéré, L., Myneni, C., Piao, R.B., S., and Thornton, P.: Carbon and Other Biogeochemical Cycles. In: *Climate Change 2013: The Physical Science Basis, Contribution of Working Group I to the Fifth Assessment Report of the Intergovernmental Panel on Climate Change*. In: Stocker, T. F., Qin, D., Plattner, G.-K., Tignor, M., Allen, S. K., Boschung, J., Nauels, A., Xia, Y., Bex, V., Midgley, P. M. (eds.) Cambridge University Press, Cambridge (2013)
- de Gouw, J.A., Veeffkind, J.P., Roosenbrand, E., et al.: Daily satellite observations of methane from oil and gas production regions in the United States. *Sci. Rep.* **10**, 1379 (2020). <https://doi.org/10.1038/s41598-020-57678-4>
- IPCC: *Climate Change 2014– Synthesis Report: Contribution of Working Groups I, II and III to the Fifth Assessment Report of the Intergovernmental Panel on Climate Change* (Geneva, Switzerland). <https://www.ipcc.ch/report/ar5/syr/> (2014)
- Kirschke, S., Bousquet, P., Ciais, P., Sauniois, M., Canadell, J.G., Dlugokencky, E.J., Bergamaschi, P., Bergmann, D., Blake, D.R., Bruhwiler, L., Cameron-Smith, P., Castaldi, S., Chevallier, F., Feng, L., Fraser, A., Heimann, M., Hodson, E.L., Houweling, S., Josse, B., Fraser, P.J., Krummel, P.B., Lamarque, J.F., Langenfelds, R.L., Le Quere, C., Naik, V., O’Doherty, S., Palmer, P.I., Pison, I., Plummer, D., Poulter, B., Prinn, R.G., Rigby, M., Ringeval, B., Santini, M., Schmidt, M., Shindell, D.T., Simpson, I.J., Spahni, R., Steele, L.P., Strode, S.A., Sudo, K., Szopa, S., van der Werf, G.R., Voulgarakis, A., van Weele, M., Weiss, R.F., Williams, J.E., Zeng, G.: Three decades of global methane sources and sinks. *Nat. Geosci.* **6**, 813–823 (2013). <https://doi.org/10.1038/ngeo1955>
- Miller, S.M., Wofsy, S.C., Michalak, A.M., Kort, E.A., Andrews, A.E., Biraud, S.C., Dlugokencky, E.J., Eluszkiewicz, J., Fischer, M.L., Janssens-Maenhout, G., Miller, B.R., Miller, J.B., Montzka, S.A., Nehrkorn, T. and Sweeney, C.: Anthropogenic emissions of methane in the United States. *Proc. Natl. Acad. Sci. USA.* **110** (50), 20018–20022 (2013). <https://doi.org/10.1073/pnas.1314392110>
- Nisbet, E.G., Fisher, R.E., Lowry, D., France, J.L., Allen, G., Bakkaloglu, S.: Methane mitigation: methods to reduce emissions, on the path to the Paris agreement. *Rev. Geophys.* **58**(2020), e2019RG000675. <https://doi.org/10.1029/2019RG000675>
- Pacala, S.W.: *Verifying greenhouse gas emissions: Methods to support international climate agreements*. National Academies Press, Washington, D.C. (2010)
- Sauniois, M., Bousquet, P., Poulter, B., Peregón, A., Ciais, P., Canadell, J.G., Dlugokencky, E.J., Etiope, G., Bastviken, D., Houweling, S., Janssens-Maenhout, G., Tubiello, F.N., Castaldi, S., Jackson, R.B., Alexe, M., Arora, V.K., Beerling, D.J., Bergamaschi, P., Blake, D.R., Brailsford, G., Bruhwiler, L., Crevoisier, C., Crill, P., Covey, K., Frankenberg, C., Gedney, N., Höglund-Isaksson, L., Ishizawa, M., Ito, A., Joos, F., Kim, H.-S., Kleinen, T., Krummel, P., Lamarque, J.-F., Langenfelds, R., Locatelli, R., Machida, T., Maksyutov, S., Melton, J.R., Morino, I., Naik, V., O’Doherty, S., Parmentier, F.-J.W., Patra, P.K., Peng, C., Peng, S., Peters, G.P., Pison, I., Prinn, R., Ramonet, M., Riley, W.J., Saito, M., Santini, M., Schroeder, R., Simpson, I.J., Spahni, R., Takizawa, A., Thornton, B.F., Tian, H., Tohjima, Y., Viovy, N., Voulgarakis, A., Weiss, R., Wilton, D.J., Wiltshire, A., Worthy, D., Wunch, D., Xu, X., Yoshida, Y., Zhang, B., Zhang, Z., Zhu, Q.: Variability and quasi-decadal changes in the methane budget over the period 2000–2012. *Atmos. Chem. Phys.* **17**, 11135–11161 (2017). <https://doi.org/10.5194/acp-17-11135-2017>
- Sauniois, M., Stavert, A.R., Poulter, B., Bousquet, P., Canadell, J.G., Jackson, R.B., Raymond, P.A., Dlugokencky, E.J., Houweling, S., Patra, P.K., Ciais, P., Arora, V.K., Bastviken, D., Bergamaschi, P., Blake, D.R., Brailsford, G., Bruhwiler, L., Carlson, K.M., Carrol, M., Castaldi, S., Chandra, N., Crevoisier, C., Crill, P.M., Covey, K., Curry, C.L., Etiope, G., Frankenberg, C., Gedney, N., Hegglin, M.I., Höglund-Isaksson, L., Hugelius, G., Ishizawa, M., Ito, A., Janssens-Maenhout, G., Jensen, K.M., Joos, F., Kleinen, T., Krummel, P.B., Langenfelds, R.L., Laruelle, G.G., Liu, L., Machida, T., Maksyutov, S., McDonald, K.C., McNorton, J., Miller, P.A., Melton, J.R., Morino, I., Müller, J., Murguía-Flores, F., Naik, V., Niwa, Y., Noce, S., O’Doherty, S., Parker, R.J., Peng, C., Peng, S., Peters, G.P., Prigent, C., Prinn, R., Ramonet, M., Regnier, P., Riley, W.J., Rosentretter, J.A., Segers, A., Simpson, I.J., Shi, H., Smith, S.J., Steele, L.P., Thornton, B.F., Tian, H., Tohjima, Y., Tubiello, F.N., Tsuruta, A., Viovy, N., Voulgarakis, A., Weber, T.S., van Weele, M., van der Werf, G.R., Weiss, R.F., Worthy, D., Wunch, D., Yin, Y., Yoshida, Y., Zhang, W., Zhang, Z., Zhao, Y., Zheng, B., Zhu, Q., Zhu, Q., Zhuang, Q.: The Global Methane Budget 2000–2017. *Earth Syst. Sci. Data* **12**, 1561–1623 (2020). <https://doi.org/10.5194/essd-12-1561-2020>
- Turner, A.J., Frankenberg, C., Kort, E.A.: Interpreting contemporary trends in atmospheric methane. *Proc. Natl. Acad. Sci. U. S. A.* **116**, 2805–2813 (2019). <https://doi.org/10.1073/pnas.1814297116>

Publisher’s Note Springer Nature remains neutral with regard to jurisdictional claims in published maps and institutional affiliations.